



Chemical Composition and Bacterial Community in Size-Resolved Cloud Water at the Summit of Mt. Tai, China

Chao Zhu¹, Jianmin Chen^{1,2,3*}, Xinfeng Wang¹, Jiarong Li¹, Min Wei¹, Caihong Xu¹, Xianmang Xu¹, Aijun Ding³, Jeffrey L. Collett, Jr.⁴

¹ Environment Research Institute, School of Environmental Science and Engineering, Shandong University, Ji'nan 250100, China

² Shanghai Key Laboratory of Atmospheric Particle Pollution and Prevention, Department of Environmental Science and Engineering, Institute of Atmospheric Sciences, Fudan University, Shanghai 200433, China

³ Institute for Climate and Global Change Research, School of Atmospheric Sciences, Nanjing University, Nanjing, Jiangsu 210008, China

⁴ Department of Atmospheric Science, Colorado State University, Fort Collins, CO 80523, USA

ABSTRACT

A three-stage collector was used to collect size-resolved cloud samples at the summit of Mt. Tai. Subsequently, analyses of pH values, water-soluble ions, and trace metals were performed and bacterial community were conducted using MiSeq amplicon sequencing. The pH values of the samples decreased as droplet sizes decreased. Sulfate (SO₄²⁻), nitrate (NO₃⁻) and ammonium (NH₄⁺) were the main secondary inorganic ions which their concentration distributed significantly different from size-resolved cloud water. The NH₄⁺ concentration was higher in smaller droplets. The SO₄²⁻ and NO₃⁻ concentrations were higher in larger droplets. The Ca²⁺ concentration increased as droplet size increased. Small droplet samples tended to have lower pH value, mainly because of the more acidic (SO₄²⁻ and NO₃⁻) and less acid-neutralizing (NH₄⁺ and Ca²⁺) components. The bacterial community in size-resolved cloud samples were firstly recognized and dominated by the genera of *Lactococcus* (average abundance 34.9%) and *Bacillus* (average abundance 34.0%). Linear discriminant analysis effect size (LEfSe) revealed differences of the bacterial community in size-resolved cloud water samples, which was probably caused by the bacterial size. Redundancy analysis suggested several minor correlations that the H₂O₂, NO₂⁻ concentrations, and trace metals exert effects on the bacterial community.

Keywords: Cloud sample; Three-stage collector; Chemical composition; Bacterial community.

INTRODUCTION

Clouds play a vital role because they serve as efficient receivers and reactors that change the physical or chemical properties of aerosol particles and trace gases (Biswas *et al.*, 2008; Li *et al.*, 2011; Boone *et al.*, 2015). Clouds are both the source and the sink of atmospheric particles. Particles in air serve as nuclei for water condensation and for the subsequent cloud droplets formation (Hao *et al.*, 2016). By contrast, droplets evaporate when the cloud dissipates, leaving particles in air (Peng, 2015). Cloud droplets are also beneficial to heterogeneous and aqueous reactions (Notholt *et al.*, 1992; Huijnen *et al.*, 2014; Hoyle *et al.*, 2015). Trace

gases and radicals react on the surface or inside of the cloud droplets, leading to changes in the composition of secondary aerosol particles (Weller and Herrmann, 2015; Whalley *et al.*, 2015).

Cloud droplets have been observed in many locations, and their chemical compositions vary depending on the droplet size (Bator and Collett, 1997; Bower *et al.*, 2000; Straub and Collett, 2002). The chemical properties of cloud droplets depend on the source, the supersaturation state, and the size and chemical composition of cloud condensation nuclei (CCN) (Van Pinxteren *et al.*, 2016). Relative studies applying two-fractions collectors demonstrated that non-volatile solute concentrations tend to be relatively high in larger drops (Menon *et al.*, 2000), and crustal species tend to be relatively low in smaller drops (Hoag and Pandis, 1999). However, observations from three droplet size fractions are limited.

Bacteria are ubiquitous in the atmosphere, with the mean concentration of approximately 1×10^4 cells m⁻³ (Elbert *et al.*, 2007; Burrows *et al.*, 2009). The bacterial communities

* Corresponding author.

Tel.: +86-531-88363711; Fax: +86-531-88361990

E-mail address: jmchen@sdu.edu.cn;

jmchen@fudan.edu.cn

contained in clouds and fogs can markedly influence processes that affect terrestrial or aquatic ecosystems (Kourtev *et al.*, 2011). Example, these bacterial communities can affect global clouds distribution and precipitation by serving as CCN and potential ice nuclei (IN) (Ariya *et al.*, 2009; Pratt *et al.*, 2009; Joly *et al.*, 2014); bacterial communities are major allergens and can be plant or animal pathogens (Peccia and Hernandez, 2006; Cao *et al.*, 2014), constituting a public concern. Abundant evidence has confirmed the diversity of the bacterial community in cloud water (Bauer *et al.*, 2003), and some studies have characterized the bacterial community (Kourtev *et al.*, 2011; Xu *et al.*, 2016) in cloud water samples. However, the influence of different cloud droplet size ranges on the bacterial community is sparse.

The North China Plain, from which many sources of anthropogenic pollutants originate and around which large tracts of farmland are located, is one of the fastest industrializing and developing areas in China. In the present study, a three-stage collector was used to collect cloud samples at Mt. Tai. The pH value and electrical conductivity (EC) were measured in situ while inorganic ions and trace metals were analyzed in the laboratory. The tendencies of size-resolved pH and size-resolved major ions in cloud water samples were investigated, and their causes were analyzed. MiSeq amplicon sequencing, redundancy analysis, and linear discriminant analysis effect size (LEfSe) were applied to investigate the bacterial diversity of the collected samples. The relationship between chemical composition and bacterial diversity was also evaluated.

EXPERIMENTAL

Site and Sampling

Mt. Tai, located in the north of Tai'ai City, Shandong Province, is the highest point in the North China Plain. Size-resolved cloud water samples were collected at a meteorological station situated at the summit of Mt. Tai (36°18N, 117°13E, 1534 m a.s.l.) (Wang *et al.*, 2011) from June 24 to August 08, 2015. In the south of Mt. Tai, plenty of farmland and many factories sited. The farmland was mainly planted with peanuts and corns in summer. And the factories contained power plants, chemical plants, and coking plants, which emitted particulate matter, acidic gases, carbon monoxide, and coal ash to the local atmospheric environment.

Size-resolved cloud water samples were collected using a three-stage Caltech Active Strand Cloud water Collector (CASCC) (Demoz *et al.*, 1996), with 50% collection efficiency cut-off diameters (D_{50}) of 22, 16, and 4 μm for stage 1, stage 2 and stage 3 respectively (Raja *et al.*, 2008; Spiegel *et al.*, 2012). Cloud droplets entering the collector were separated to different size fractions and captured by the given impaction obstacles. A 500-mL pre-cleaned closed polyethylene collection bottle was used in each stage to accumulate the size-resolved cloud water samples. Generally, only one set of samples could be collected during one cloud event, and the lowest sample volume was obtained in stage 2. If rain was expected, the collector was deployed with a downward facing inlet to prevent rain water from entering the three-stage CASCC. Cloud events were distinguished

by a 6 h non-cloudy period. After sampling, the three-stage collector was cleaned using high-purity deionized water ($> 18.2 \text{ M}\Omega$). Field blanks were collected and analyzed following the same processes applied for cloud water samples.

The cloud droplet number concentration and the liquid water content were measured using a droplet size spectrometer (FM-120) with a time resolution of 1s. The $\text{PM}_{2.5}$ concentration was obtained using a Beta attenuation and optical analyzer (Thermo Scientific, model 5030 SHARP monitor).

The Hybrid Single-Particle Lagrangian Integrated Trajectory (HYSPPLIT) developed by National Oceanic and Atmospheric Administration (NOAA) was applied to investigate the origins of the cloud events. The 72-h backward trajectories of cloud events were calculated every 12 h arriving at Mt. Tai, with the height of 1534m a.s.l. and four clusters were classified.

Chemical Analysis of Cloud Samples

The pH and the EC values of the cloud samples were measured immediately after sampling by a pH/conductivity analyzer (pH/COND/TEMP METER, 6350). And the measure accuracy and error were presented in supplement. The formaldehyde (HCHO), hydrogen peroxide (H_2O_2) and sulfur(IV) [S(IV)] concentrations were measured on-site (Collett *et al.*, 1998). HCHO was determined using the acetylacetone spectrophotometric method. H_2O_2 was determined using the fluorescence standard curve method. S(IV) was measured using the pararosaniline UV-visible spectrophotometric method.

The inorganic ions of sodium (Na^+), ammonium (NH_4^+), potassium (K^+), magnesium (Mg^{2+}), calcium (Ca^{2+}), fluorine (F^-), chlorine (Cl^-), nitrite (NO_2^-), sulfate (SO_4^{2-}) and nitrate (NO_3^-), were determined using ion chromatography (Dionex, ICS-90) after 1:10 dilution of the samples and subsequent filtration. Fig. 1 presents the balance of inorganic anions versus cations, including $[\text{H}^+]$. Most samples exhibited a favorable ion balance, indicating the high quality of measurement.

Trace metals, namely aluminum (Al), vanadium (V), chromium (Cr), manganese (Mn), iron (Fe), cobalt (Co), nickel (Ni), copper (Cu), zinc (Zn), arsenic (As), selenium (Se), cadmium (Cd) and barium (Ba) were measured by inductively coupled plasma mass spectrometry (ICP-MS, Agilent 7500a). Samples were pretreated by acidification with 1% (v/v) nitric acid to reduce the adsorption from the inner wall of container. Then the samples were stored at 4 degrees until analysis. Li, Sc, Ge, Rh, Tb and Lu were used as internal standard and the recovery rates were all in the range of 90%–110%. Black samples were also prepared as above and analyzed. The detection limit of ICP-MS analysis for the trace metals were calculated as 3 times the standard deviation of the 6 blank values (Table 3) (Li *et al.*, 2015).

DNA Extraction and Polymerase Chain Reaction Amplification

Microbial DNA was extracted from cloud water samples using the E.Z.N.A.[®] Soil DNA Kit (Omega Bio-tek, Norcross, GA, USA) according to the manufacturer's protocols. The

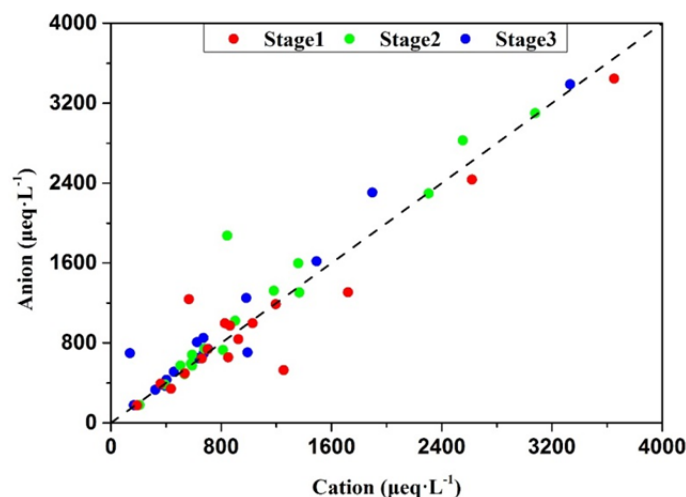


Fig. 1. Ion balance on an equivalent basis for cations and anions. Dashed line corresponds to 1:1.

V4-V5 region of the bacterial 16S ribosomal RNA gene were amplified by using polymerase chain reaction (PCR) (95°C for 3 min, followed by 27 cycles at 95°C for 30 s, 55°C for 30 s, 72°C for 45 s and a final extension at 72°C for 10 min) with the primers 515F 5'-GTGCCAGCMGCCGCGG-3' and 907R 5'-CCGTC AATTCMTTTRAGTTT-3'; 8-bp barcodes unique to each sample were used. The PCR reactions were performed in triplicate in a 20 µL mixture containing 4 µL of 5 × FastPfu Buffer, 2 µL of 2.5 mM dNTPs, 0.8 µL of each primer (5 µM), 0.4 µL of FastPfu Polymerase, and 10 ng of template DNA. Finally, dd H₂O was added to fill out the final volume to 20 µL.

Illumina MiSeq Sequencing and Processing of Sequencing Data

Amplicons were extracted from 2% agarose gels and purified using an AxyPrep DNA Gel Extraction Kit (Axygen Biosciences, Union City, CA, USA) according to the manufacturer's instructions and quantified using QuantiFluor™ -ST (Promega, USA). The purified amplicons were pooled in equimolar amounts and paired-end sequenced (2 × 250) on an Illumina MiSeq platform according to standard protocols. The raw reads were deposited to the NCBI Sequence Read Archive (SRA) database (Accession Number: SRX2191488).

Raw fastq files were demultiplexed and quality-filtered using QIIME (version 1.17) with the following criteria: (i) the 300-bp reads were truncated at any site receiving an average quality score of less than 20 over a 50-bp sliding window, and truncated reads shorter than 50-bp were discarded; (ii) the reads with exact barcode matching or two-nucleotide mismatch in primer matching and those containing ambiguous characters were removed; and (iii) only sequences with overlap longer than 10-bp were assembled according to their overlap sequence. Reads that could not be assembled were discarded.

Operational Taxonomic Units (OTUs) with 97% similarity were clustered using UPARSE (version 7.1 <http://drive5.com/uparse/>), and chimeric sequences were identified and

removed using UCHIME. The taxonomy of each 16S rRNA gene sequence was analyzed using the RDP Classifier (<http://rdp.cme.msu.edu/>) against the silva (SSU115)16S rRNA database by applying a confidence threshold of 70% (Amato *et al.*, 2013). The relationships between environmental variables and the cloud water bacterial community were analyzed using redundancy analysis (RDA) with CANOCO software (version 4.56, Microcomputer Power, Inc., Ithaca, NY, USA). LefSe analysis (Segata *et al.*, 2011) was applied to identify the phylogenetically coherent members of the bacterial community. LefSe analysis was used to detect the differential abundant features in the three cloud droplet size fractions (n = 10 per category), then to test the phylogenetic consistency, and finally to estimate the effect size of each differentially abundant feature by using linear discriminant analysis (LDA). Moreover, the LDA score of 3.0 was chosen as the threshold for discriminative features.

RESULTS AND DISCUSSION

The pH and Chemical Composition of Cloud Water Samples at Mt. Tai

Table 1 summarizes the basic conditions of all 17 sets of cloud samples collected during 10 cloud events at Mt. Tai. Most of the cloud events formed in late night and dissipated during the morning hours. Inside, some long events lasted for almost 2 days (43.8 h). The number concentration and the liquid water content of each cloud event ranged from 293 to 1396 cm⁻³ and from 0.065 to 0.420 g m⁻³, respectively. In the process of sampling, once one collection bottle of any stage reached to the maximum volume, all the collecting bottles were unslung and one set of size-resolved cloud water samples were finished. And if the cloud event continued, another set of empty collection bottles would be applied to the following sampling within 5 min. During cloud events E-1 to E-3, multiple sets of samples were collected. During cloud events E-4 to E-10, only one set of samples was collected. Table 2 provides a summary of different chemical compositions. The average values and volume weighted

Table 1. Sampling times of the samples during cloud events with mean liquid water content (LWC), droplet number concentration (NC) and number of sample sets (NSS).

Sample ID	Sampling Time	Duration (h)	PM _{2.5} (μg m ⁻³)	NC (cm ⁻³)	LWC (g m ⁻³)	NSS
E-1	24 June, 05:58–24 June, 19:45	13.8	5.1	866	0.245	2
E-4	29 June, 11:00–29 June, 15:30	4.5	12.8	1021	0.199	1
E-5	30 June, 17:30–01 July, 08:40	15.2	9.3	877	0.234	1
E-6	18 July, 17:40–18 July, 21:20	3.7	7	956	0.251	1
E-7	19 July, 12:50–19 July, 17:30	4.7	23.6	1048	0.354	1
E-8	22 July, 19:00–23 July, 05:25	10.4	26.3	389	0.065	1
E-2	27 July, 23:00–29 July, 12:26	37.4	7.8	835	0.240	4
E-9	29 July, 22:28–30 July, 05:11	6.7	4	1396	0.420	1
E-3	01 August, 23:45–03 August, 19:34	43.8	5.8	1219	0.325	4
E-10	05 August, 21:45–06 August, 08:30	10.8	0.7	293	0.150	1

Table 2. Summary of determined cloud water solute concentrations.

Compound	Unit	Range			Mean			VWM		
		Stage 1	Stage 2	Stage 3	Stage 1	Stage 2	Stage 3	Stage 1	Stage 2	Stage 3
pH		3.8–6.3	3.7–6.1	3.6–6.6	4.87	4.80	4.68	4.86 ^a	4.70 ^a	4.67 ^a
EC	μS cm ⁻¹	30–501	29–496	26–547	158	170	155	157	183	157
NH ₄ ⁺	μmol L ⁻¹	76–1826	68–2246	71–2938	511	683	697	548	739	688
K ⁺	μmol L ⁻¹	2.4–38	2.4–65	1.3–53	15	18	15	16	20	14
Ca ²⁺	μmol L ⁻¹	10–817	26–395	6–297	244	248	50	212	118	46
Na ⁺	μmol L ⁻¹	3.9–102	9.1–80	4.3–54	32	30	18	29	27	18
Mg ²⁺	μmol L ⁻¹	BDL–49	6–36	BDL–20	19	17	5	16	15	4
NO ₃ ⁻	μmol L ⁻¹	56–1073	56–958	40–1003	307	323	252	306	353	244
SO ₄ ²⁻	μmol L ⁻¹	56–1025	57–965	53–1081	305	357	300	302	387	293
Cl ⁻	μmol L ⁻¹	2.4–173	7.4–247	3.3–160	56	64	43	57	71	42
F ⁻	μmol L ⁻¹	BDL–147	1.4–116	13–91	49	41	38	40	32	36
NO ₂ ⁻	μmol L ⁻¹	0.9–12	1.1–12	0.9–9.4	4.8	4.9	3.8	4.6	5.2	3.5
HCHO	μmol L ⁻¹	BDL–66	BDL–64	BDL–80	24	25	27	19	18	24
S(IV)	μmol L ⁻¹	BDL–73	BDL–72	BDL–86	17	19	22	11	12	14
H ₂ O ₂	μmol L ⁻¹	1.7–37	2.2–26	3.7–37	12	9.4	15	12	8.3	15

EC: electrical conductivity; VWM: volume-weighted mean concentration (The formula is described in the supplement); a: VWM pH were derived from VWM H⁺ concentration; BDL: below detection limit.

mean (VWM) values of pH and inorganic ions were derived for all cloud samples.

Fig. 2 illustrates all pH values for the 10 cloud events. The pH values of all cloud samples ranged between 3.6 and 6.6, with the lowest value in stage 3, E-5, and the highest value in the stage 3, E-2.3. The maximum pH difference in one set of samples reached up to 0.97 in E-2.3. 39.2% of samples had the pH value lower than 5.6 and 9.8% of samples had the pH value lower than 4.5. The VWM pH of all collected samples was 4.74, which was extremely close to the value at Hokkaido, Japan (Yamaguchi *et al.*, 2015), and was higher than preceding cloud observation results (3.86 in the period of 2007–2008) at the same site (Guo *et al.*, 2012). These results indicating an increased pH tendency in the Mt. Tai cloud water. Ten sets of samples exhibited the lowest pH value in stage 3 whereas 13 sets of samples exhibited the highest pH value in stage 1, indicating that small droplets tended to be more acidic than large droplets. Hence, the dominant tendency found for size-dependent pH values was that pH values decreased with decreasing droplet size.

The EC values of cloud water collected during this study

ranged from 26 to 547 μS cm⁻¹. The VWM values for stage 1, stage 2, and stage 3, were 157, 183, and 157 μS cm⁻¹ respectively. Regarding the ionic compositions, this study found that cloud water collected at Mt. Tai mainly contained NH₄⁺, SO₄²⁻, NO₃⁻ and Ca²⁺, accounting for approximately 90% of the total determined ionic compositions. On average, NH₄⁺ accounted for 26.1%, 31.5% and 38.6% of the total ions in stage 1, stage 2 and stage 3. Given that Mt. Tai is surrounded by large tracts of farmland and livestock, the finding that NH₄⁺ was the most abundant cation in Mt. Tai cloud water sample was reasonable. Similar to the concentrations found in previous Mt. Tai campaigns (Guo *et al.*, 2012), Ca²⁺ was detected at relatively high concentrations (424, 236, and 92 μeq L⁻¹ for stage 1, stage 2 and stage 3, respectively) in cloud water samples. SO₄²⁻ was the most abundant anion in the cloud water samples, with VWM concentrations of 603, 773, and 585 μeq L⁻¹ for stage 1, stage 2 and stage 3, respectively. NO₃⁻ was the second most abundant anion in the cloud water samples, with a VWM concentration no more than 51% of the SO₄²⁻ concentration. In previous Mt. Tai campaigns (Wang *et al.*, 2011; Guo *et al.*, 2012), the VWM concentrations of SO₄²⁻ were measured

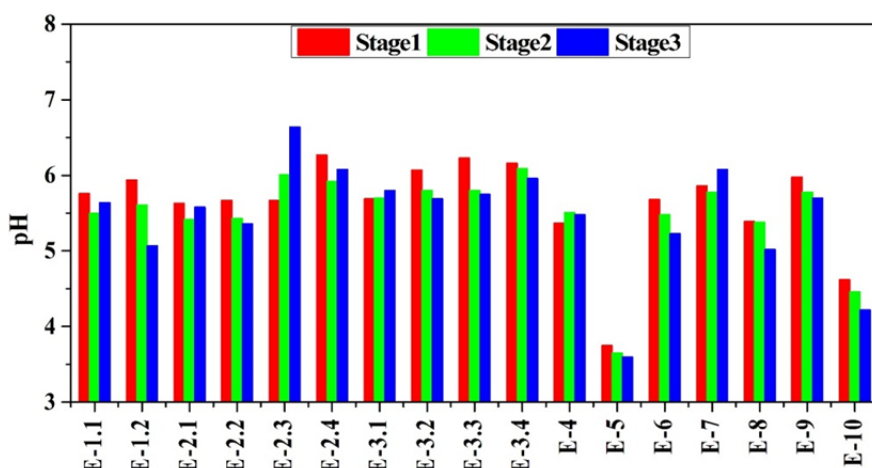


Fig. 2. Size-resolved pH value. In cloud event E-1 to E-3, multiple sets of samples were distinguished by numbers, example E-1.1 and E-1.2 respectively represented the first and second set of samples in E-1.

as more than $1000 \mu\text{eq L}^{-1}$. However, in our study, much lower concentrations were detected. The reason was mainly because the China government donated lots of efforts to SO_2 emission reduction so the precursor of sulfate decreased. The data published on the Ministry of Environment Protection of the People's Republic of China confirmed that 24.5% (6.09 million tons) of SO_2 was reduced from 2007 to 2015. And the data published on the Ministry of Environment Protection of Shandong Province also confirmed that 16.5% (0.3 million tons) of SO_2 was reduced from 2011 to 2015 (Fig. S1). Meanwhile, these low SO_4^{2-} concentrations may also be caused by our sampling time, which was from late June to the early August in summer, during when the residential heating had not yet been initiated. Thus, SO_4^{2-} coming from the conversion of SO_2 from the coal combustion was not accounted for in our data. Moreover, rain and cloud events are more frequent in summer than in other seasons; thus, the scavenging effect would favor for the lower SO_4^{2-} concentration.

The concentrations of the major ions SO_4^{2-} , NO_3^- and NH_4^+ in the three droplet size fractions varied significantly between different cloud events. By contrast, these concentrations were similar in the same cloud event, particularly in E-3 samples. Mostly, the ratio between the highest and lowest concentration of major ion in one set of samples were within a factor of 3. As shown in Fig. 3, NH_4^+ had a higher concentration in smaller (stage 2 and stage 3) droplets in almost all samples (16 of 17 sets of samples). In most cases, SO_4^{2-} had the highest concentrations in stage 2 (12 of 17 sets of samples) but the lowest concentration in stage 3 (13 of 17 sets of samples). NO_3^- had a higher concentration in larger (stage 1 and stage 2) droplets, with the highest concentrations in 9 sets in stage 2 and 6 sets in stage 1. The Ca^{2+} concentration was widely different in the three size fractions, and VWM concentration in stage 2 and stage 1 were twice and four times greater than that in stage 3 (Fig. 3). Although Mg^{2+} accounted for only less than 2%, the concentration of Mg^{2+} exhibited a tendency similar to Ca^{2+} ; the concentration in stage 3 was less than a quarter of that in other stages and some

concentrations even below detection limit.

Table 3 summarizes the average concentrations of trace metals in cloud water samples. Zn was the dominant trace metal with an average concentration higher than $500 \mu\text{g L}^{-1}$ for each stage. The other three trace metals in the first four followed the order: $\text{Al} > \text{Fe} > \text{Mn}$. Cu and Ba showed similar concentrations (approximately $25 \mu\text{g L}^{-1}$ for each stage). By contrast, V, Cr, Ni, As, Se and Cd were all between $1 \mu\text{g L}^{-1}$ and $10 \mu\text{g L}^{-1}$. The trace metal Co was detected at the lowest concentration (less than $1 \mu\text{g L}^{-1}$). The concentrations of the trace metals were the same order of magnitude as the previous data in Mt. Tai (Liu *et al.*, 2012). But the concentration levels were much higher than in Mt. Schumcke (Fomba *et al.*, 2015) and Mt. Brocken (Plessow *et al.*, 2001) in Europe. Especially, V, Mn, Se and As in this study were one order of magnitude higher than in Mt. Schumcke.

At Mt. Tai, more fine particles existed in summer and the main compounds of these fine particles were SO_4^{2-} , NH_4^+ and NO_3^- (Deng *et al.*, 2011). When these fine particles served as CCN and formed cloud events, major ions would concentrate in smaller size droplets. Moreover, smaller droplets had more specific surface area for facilitating the mass transfer of soluble gases, such as SO_2 , NO_x and NH_3 . Thus the major ions were concentrated in smaller size droplets. In the literature, the droplet size increased with decreasing concentrations of major ions or minimum major ions in stage 2, as observed in Mt. Schumcke (Van Pinxteren *et al.*, 2016). Raja and co-workers (Raja *et al.*, 2008) found that major ions were concentrated in small droplets. The tendencies of Ca^{2+} and Mg^{2+} may be explained by their source, soil dust. Soil dust has a much larger size distribution (Bi *et al.*, 2013) than the droplets collected in stage 2 and stage 3, which meant if the soil dust participated in the cloud process, the larger droplets were more possible to contain soil dust components, and if the droplets were too small, it was less likely to find the soil dust elements inside. These results strongly suggested that the size distribution and chemical composition of CCN may be the causes of the chemical heterogeneity of droplets at Mt. Tai. Other minor

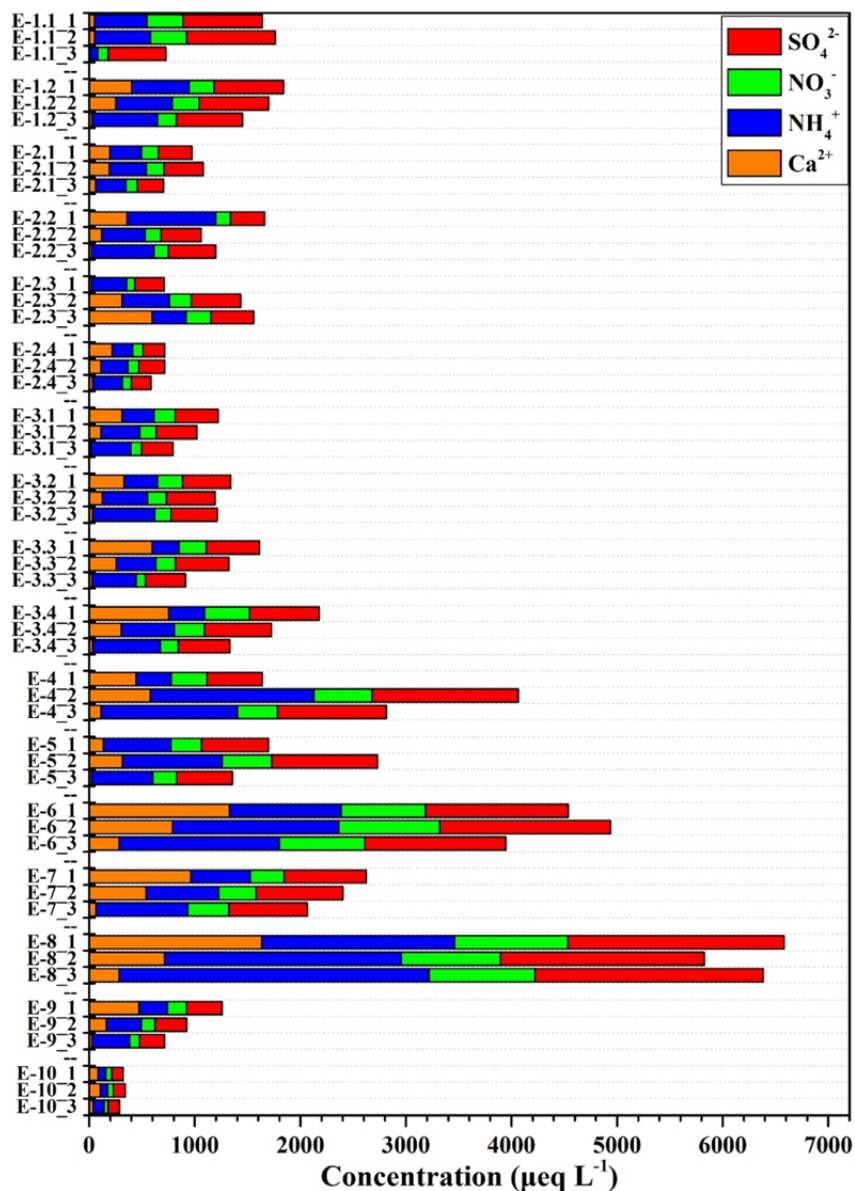


Fig. 3. Size-resolved concentrations of sulfate, nitrate, ammonium and calcium. Stages in the same set of samples were distinguished by numbers, example E-1.1_1, E-1.1_2 and E-1.1_3 respectively represented samples of stage 1, stage 2 and stage 3 from E-1.1.

Table 3. Summary of averaged trace metals concentrations and detection limit.

Compound (µg L ⁻¹)	Stage 1	Stage 2	Stage 3	Detection limit
Al	249	267	254	2.22
V	3.0	3.1	3.2	0.02
Cr	2.7	2.0	2.4	0.05
Mn	42.0	44.4	41.1	0.02
Fe	106	119	118	0.30
Co	0.3	0.2	0.2	0.01
Ni	2.3	2.7	2.3	0.06
Cu	23.4	26.7	25.2	0.07
Zn	554	529	507	0.26
As	5.6	6.7	7.2	0.01
Se	4.5	5.3	5.8	0.03
Cd	1.4	1.5	1.7	0.01
Ba	27.2	27.2	21.8	0.09

ions did not exhibit regular size distribution in our study. But in available literature data (Collett *et al.*, 1995; Raja *et al.*, 2009; Van Pinxteren *et al.*, 2016), minor ions were found diverse size distribution profiles and this may depend on sampling sites and compound species.

The pH of cloud droplets was mainly determined by the combined effect of acidic and acid-neutralizing components. The VWM pH values for stage 1, stage 2 and stage 3 were 4.86, 4.70 and 4.67 respectively. Stage 3 samples tended to have lower pH value, whereas stage 1 samples tended to have higher pH value. This result was caused by the more acidic components in smaller droplets and the more acid-neutralizing components in larger droplets.

SO_4^{2-} and NO_3^- were found to be the main acidic components. By contrast, NH_4^+ and Ca^{2+} played a crucial role in cloud water neutralization (Hutchings *et al.*, 2009). Comparison of the pH values between stage 1 and stage 3 by using VWM concentrations revealed that although acidic components in stage 1 exceeded those in stage 3 with VWM concentrations of $18 \mu\text{eq L}^{-1}$ for SO_4^{2-} and $62 \mu\text{eq L}^{-1}$ for NO_3^- , stage 1 samples (VWM pH = 4.86) still had higher pH value than stage 3 samples (VWM pH = 4.67). This finding is because the concentration of Ca^{2+} in stage 1 ($424 \mu\text{eq L}^{-1}$) was higher than that in stage 3 ($92 \mu\text{eq L}^{-1}$). Although NH_4^+ concentration in stage 3 ($688 \mu\text{eq L}^{-1}$) exceeded that in stage 1 ($548 \mu\text{eq L}^{-1}$), overall, acid-neutralizing components in stage 1 exceeded those in stage 3 with the value of $192 \mu\text{eq L}^{-1}$. Moreover, this was also far large than the deficient $80 \mu\text{eq L}^{-1}$ of acidic components.

The Ca^{2+} concentration in stage 1 exceeded that in stage 2 with the value of $188 \mu\text{eq L}^{-1}$. However, NH_4^+ concentration in stage 2 surpassed that in stage 1 with the value of $191 \mu\text{eq L}^{-1}$. Thus the neutralizing effects were almost the same in the two size fractions. However, the effect from

acidic components was much greater in stage 2, which had $217 \mu\text{eq L}^{-1}$ more of acidic compounds ($170 \mu\text{eq L}^{-1}$ of SO_4^{2-} and $47 \mu\text{eq L}^{-1}$ of NO_3^-) than stage 1. Therefore, stage 1 (VWM pH = 4.86) had higher pH values contrast to stage 2 (VWM pH = 4.70).

Three-day air mass backward trajectories were applied to estimate the potential source regions and pathway of air pollutants (Fig. 4). According to the source direction, air masses were classified into four clusters. Cluster Southwest (contained E-2, 3, 9, and 10) mainly originated from continent area Hunan and Jiangxi Province. Cluster East (contained E-4, 6, 7, and 8) mainly came from the East China Sea and traveled through the north Jiangsu Province. Samples in Cluster East had higher Cl⁻ concentration (Fig. 4(c)) than others, which consisted well with the marine source. Cluster East and Cluster Southwest were similar that they all arrived at the Mt. Tai from the south where factories and plants located. But on average, the major ions concentrations in Cluster East were much higher than in Cluster Southwest (Fig. 4(b)). Partly or all of the following reasons may explained the phenomenon: i) the air mass from the east received pollutants in Jiangsu Province; ii) the air mass from the east contained more moisture, which availed to the conversion of the secondary inorganic ions.

Air mass that generated near the ground in E-5 was Cluster Local because it was traveling and revolving around Mt. Tai. However, the cloud water samples in E-5 had the lowest pH values in each stage (3.75 in E-5.1, 3.70 in E-5.2 and 3.60 in E-5.3) for it passed through the frequent acidic precipitation area, Beijing-Tianjin-Hebei region (Wang *et al.*, 2012). Air mass in E-1 was Cluster Northwest, for it came from the northwest part of China. Usually, the air mass from this direction would contain crustal particles and lead higher pH values in samples (Wang *et al.*, 2011).

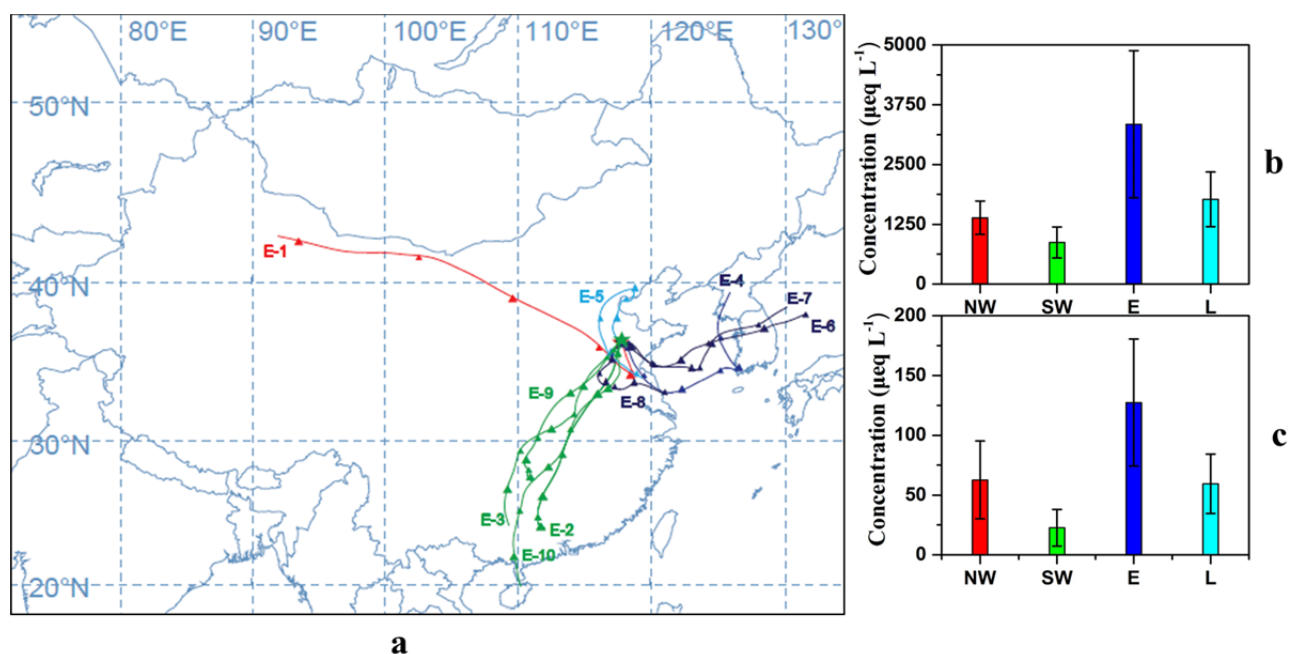


Fig. 4. (a) Three-day backward trajectories arriving at Mt. Tai; (b) Averaged major ions (including ammonium, sulfate, and nitrate) concentration of four clusters; (c) Averaged chloride concentration of four clusters.

But in our study, E-1 samples did not show these features as the PM_{2.5} concentration only 5.1 µg m⁻³, the reason could be the original altitude the air mass formed was too high (more than 6 km).

Bacterial Community in Cloud Water Samples at Mt. Tai

Given the low volume of stage 2 samples, it was difficult to obtain sufficient quantity for bacterial community analysis. Therefore, bacterial community analysis was conducted for only 10 of 17 sets of samples. Fig. 4 presents the bacterial diversity in terms of phylum and genus levels. In 30 cloud water samples from the 10 sets, the mean coverage was 0.9988, indicating adequate sequencing. Overall, 30065–43674 sequences representing 157–299 OTUs were obtained. The average number of OTUs was 210 per sample. Estimators of alpha diversity were used to assess the differences in bacterial community structure in the cloud water samples. At 97% similarity, the chao1 index ranged from 185 to 339, and the Shannon diversity index ranged from 1.83 to 2.98. Compared with the chao1 index in particulate matter (2585–12067) (Gou et al., 2016) and Shannon diversity index in aerosol (2.3–3.6) (Fahlgren et al., 2011), the diversity of the bacterial community in cloud water samples was relatively low.

The relative abundance exhibited a considerably parallel distribution in the cloud water samples. The dominant microbial groups were phyla Firmicutes, Proteobacteria, Bacteroidetes, Actinobacteria, and Fusobacteria. These five phyla accounted for 99.8% of the total OTUs. The averaged relative abundance of the dominant phylum, Firmicutes, was 80.5%, and those of Proteobacteria, Bacteroidetes, Actinobacteria, and Fusobacteria were 17.4%, 1.2%, 0.46% and 0.23%, respectively. At the genus level, the dominant bacterial groups and the mean relative abundance were: *Lactococcus* (34.9%), *Bacillus* (34.0%), *Pseudomonas* (5.2%), *Streptococcus* (4.7%), *Massilia* (3.7%), *Methylobacterium* (2.9%) and *Leuconostoc* (2.1%), accounting for 87.5% of the total OTUs. We compared the bacterial phyla identified in this study with those in previous studies. These five phyla were also found in aerosol particles (Bowers et al., 2016) and other aquatic samples, such as lake water samples (Zeng et al., 2014), rain water samples (Evans et al., 2009; Kaushik et al., 2013; Peter et al., 2014) and river water samples (Kovatch and Schultz, 2013). But in the different kinds of samples, the dominant bacteria phylum was diverse and the relative abundance of the same bacteria phylum differed greatly (Table S4). In other cloud water studies, similar genera were revealed, but the relative abundance varied a lot. For example: the genus *Pseudomonas* dominated the cloud water bacterial community in puy de Dome (Vaïtilingom et al., 2012) and Hebrides (Ahern et al., 2007), but the relative abundance of this genus was only 5.2% in our study.

Bacteria from the dominant phylum Firmicutes, which affiliated to the genus *Bacillus* can form resistance spores (Vaïtilingom et al., 2012) that enhance survival rates under conditions such as low nutrient levels or chemical damage. Thus, expectedly, this phylum was dominant in the bacteria communities in the cloud water samples. The genus

Lactococcus in the phylum Firmicutes and the genera *Pseudomonas* and *Methylobacterium* in the phylum Proteobacteria were commonly found on leaf-surface environment (Casalta and Montel, 2008; Morris et al., 2008; Redford et al., 2010), which was the type of environment provided by vegetation growing in the summer on Mt. Tai. Some taxa had potential ecological roles were identified. *Pseudomonas* (5.2%) had the potential of Fe(II) oxidization and Fe oxide precipitation (Liu et al., 2013). *Acinetobacter* (0.73%) and *Comamonas* (0.02%), belong to phylum Proteobacteria, played a key process for the Sb(III) oxidization (Lee, 2015). Stains in the genus *Sphingomonas* (0.69%) and *Pseudomonas* (5.2%) were correlated to the degradation of atmospheric organic matter (formate, acetate, etc.) (Amato et al., 2007). Beyond that, *Acinetobacter ursingii* (0.26%) was confirmed as an opportunistic human pathogen for causing bacteremia (Loubinoux et al., 2003).

Thirteen phylogenetic consistent units were identified as significant discriminators for stage 1, stage 2 or stage 3 (n = 10 per stage) (Fig. 5). Although bacterial community analysis exhibited general agreement for the dominant species, phylogenetic groups, and overall diversity, some low content OTUs differed considerably in size-resolved cloud water samples. The genus *Bacteroides*, which was the only genus from the family Bacteroidaceae in our samples, was the characteristic group in stage 1, the large droplet size fraction. The phylum Actinobacteria was the characteristic group in stage 3. And *Pedobacter* was distinctive feature of the stage 2.

The reported bacterial sizes (W × L) for *Bacteroides* were 0.5 × 2–6 µm (Buchanan et al., 1994) for stage 1. For stage 3, six genera were found in the phylum Actinobacteria, including *Arthrobacter* and *Micrococcus*. Typical bacterial species of *Arthrobacter* and *Micrococcus* and the dimensions from the literature were: *A.globiformis* [φ = 0.6–0.8 µm (for coccus) or 0.5–0.8 × 1–4 µm (for bacillus)], *A.simplex* (0.4–0.5 × 0.5–0.8 µm), *M.luteus* (φ = 1.0–2.0 µm), *M.roseus* (φ = 1.0–2.5 µm), and *M.varians* (φ = 1.0–1.5 µm) (Buchanan et al., 1994). As shown above, the bacteria that were the significant group in stage 1 had a larger size than those in stage 3, and the bacillus with a longer length in stage 1 may serve as larger CCN compared with the coccus and bacillus in stage 3. Therefore, the significant groups in the stages were probably caused by the size of bacteria serving as CCN.

Influence of Environmental Factors on Bacterial Community

RDA was used to evaluate the relationships between environmental factors and cloud droplet bacterial community, and the result was illustrated in Fig. S2. The cloud water samples from the same cloud event were clustered much closer than the samples from different cloud events, especially for samples in E-3 and E-4.

Given the limited samples (10 sets) and volumes collected in the study, we did not find markedly correlation between chemical composition and bacterial community. But several minor correlations were still seen. All environmental factors explained 74.1% of the total variance. The two principal

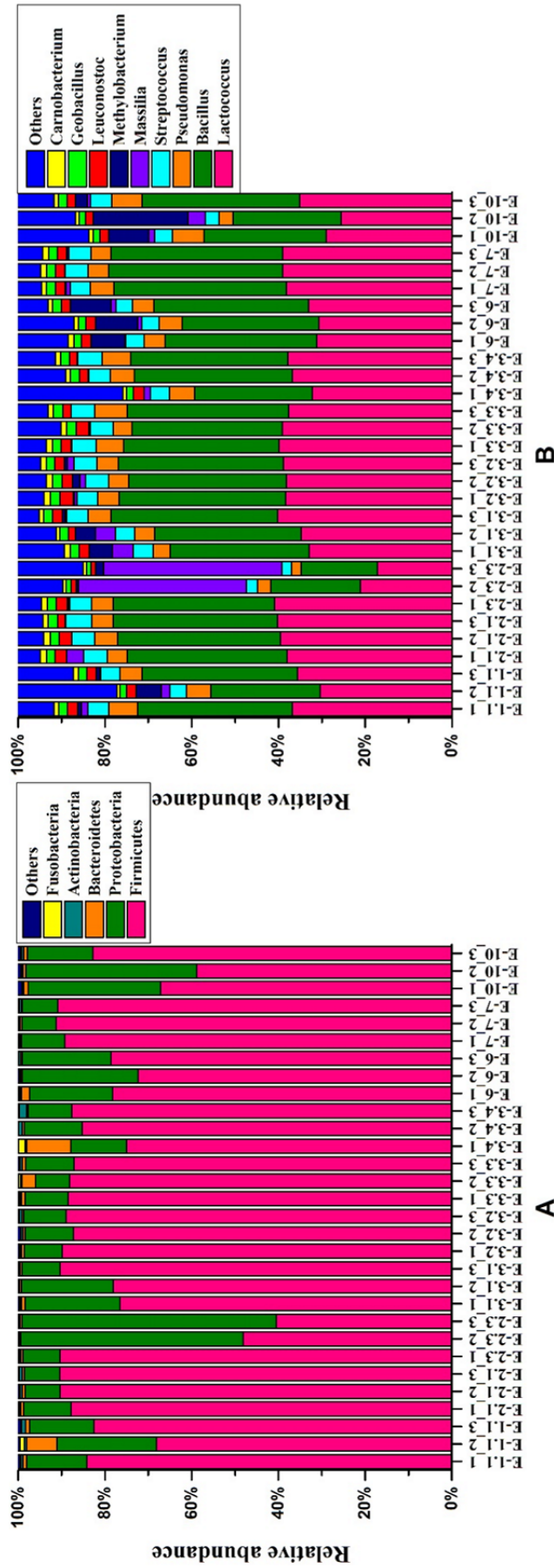


Fig. 5. Relative abundance of bacterial community in the cloud samples. A: phylum level, B: genus level.

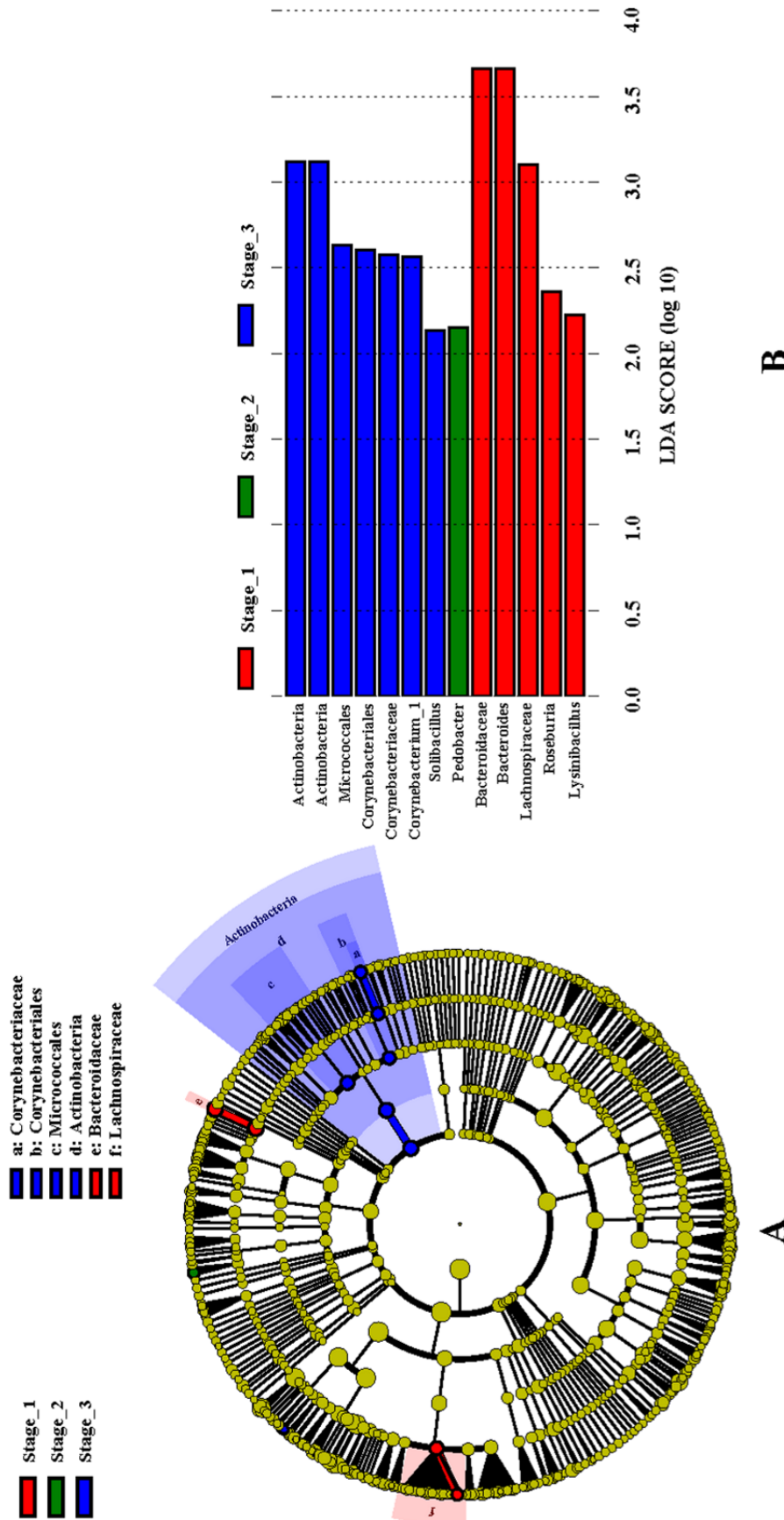


Fig. 6. LEfSe analysis results. A: Output of the LEfSe cladogram, which identified taxonomically consistent differences between stage 1, stage 2 and stage 3 community members. Taxa with nonsignificant differences are presented as yellow circles and the diameter of the circles are proportional to relative abundance. B: LDA score.

components, PC1 and PC2 that were extracted by the algorithm significantly explained 54.0% and 18.6% of the result respectively. The NO_2^- concentration positive correlated with PC1, with the coefficient of 0.194. By contrast, H_2O_2 concentration showed negative correlation, with a coefficient of -0.327 . Trace metals are essential micro-nutrients for microorganisms and participate in biogeochemical cycles, which also affected the microbial community. In this study, Cr showed positive correlation with PC1, with the factor of 0.198. Concurrently, Cd and Co showed negative correlation with PC1, with the factors of -0.192 and -0.119 , respectively.

The species in the genus *Bacillus* (*B. weihenstephanensis*) can express nitrate reductase enzyme for reducing NO_3^- to NO_2^- (Seenivasagan et al., 2016). Some other species in the genus *Bacillus* exhibited chromium-reducing ability, enabling them to survive and resist toxicity from Cr (Wani et al., 2007; Ahemad, 2015), which was consistent with the correlation factor (0.357) between PC1 and *Bacillus*. Firmicutes was not tolerant toward Cd (Lorenz et al., 2006), together with the fact that cobalt is toxic to microorganisms (Norberg and Molin, 1983) and the bactericidal effect of H_2O_2 (Forstrom and Wardle, 1980; Shintani, 2009), these factors exhibited a negative correlation with PC1.

CONCLUSIONS

In this study, a three-stage collector was used to collect size-resolved cloud water samples at Mt. Tai in the summer of 2015 to investigate chemical composition and bacterial diversity. The pH values of cloud water and the soluble ions exhibited size dependence. The pH value decreased with decreasing droplet size, with VWM average of 4.86 for stage 1, 4.70 for stage 2, and 4.67 for stage 3. The existences of more acidic and less acid-neutralizing substances led to lower pH value in smaller cloud droplets. The NH_4^+ was more abundant in smaller droplets, whereas SO_4^{2-} and NO_3^- were more abundant in larger droplets. The Ca^{2+} and Mg^{2+} concentrations also decreased with the decreasing droplet size, and the concentrations in small droplets were extremely low.

The dominant taxa and the relative abundances were similar [*Lactococcus* (17.2%–41.0%) and *Bacillus* (17.5%–40.1%)] in each sample, but LEfSe analysis revealed disparity in bacterial community in size-resolved cloud water samples. The phylum Actinobacteria was the characteristic group for stage 3 samples. The families Bacteroidaceae and Lachnospiraceae characterized stage 1 samples. Moreover, the genus *Pedobacter* was distinctive feature of stage 2 samples. The size of these bacteria might affect the size-dependence distribution of bacterial community.

ACKNOWLEDGMENTS

This work was supported by Taishan Scholar Grant (ts20120552), the National Natural Science Foundation of China (Nos. 41375126, 21190053, 21177025), Cyrus Tang Foundation (No. CTF-FD2014001), Ministry of Science and Technology of China (2016YFC0202701, 2014BAC22B01), Strategic Priority Research Program of the Chinese Academy

of Sciences (Grant No. XDB05010200).

SUPPLEMENTARY MATERIAL

Supplementary data associated with this article can be found in the online version at <http://www.aaqr.org>.

REFERENCE

- Ahemad, M. (2015). Enhancing phytoremediation of chromium-stressed soils through plant-growth-promoting bacteria. *J. Genet. Eng. Biotechnol.* 13: 51–58.
- Ahern, H.E., Walsh, K.A., Hill, T.C.J. and Moffett, B.F. (2007). Fluorescent pseudomonads isolated from Hebridean cloud and rain water produce biosurfactants but do not cause ice nucleation. *Biogeosciences* 4: 115–124.
- Amato, K.R., Yeoman, C.J., Kent, A., Righini, N., Carbonero, F., Estrada, A., Gaskins, H.R., Stumpf, R.M., Yildirim, S. and Torralba, M. (2013). Habitat degradation impacts black howler monkey (*Alouatta pigra*) gastrointestinal microbiomes. *ISME J.* 7: 1344–1353.
- Amato, P., Demeer, F., Melaouhi, A., Fontanella, S., Martinbiesse, A.S., Sancelme, M., Laj, P. and Delort, A.M. (2007). A fate for organic acids, formaldehyde and methanol in cloud water: Their biotransformation by micro-organisms. *Atmos. Chem. Phys.* 7: 4159–4169.
- Ariya, P., Sun, J., Eltouny, N., Hudson, E., Hayes, C. and Kos, G. (2009). Physical and chemical characterization of bioaerosols—Implications for nucleation processes. *Int. Rev. Phys. Chem.* 28: 1–32.
- Bator, A. and Collett, J.L. (1997). Cloud chemistry varies with drop size. *J. Geophys. Res.* 102: 28071–28078.
- Bauer, H., Giebl, H., Hitznerberger, R., Kasper-Giebl, A., Reischl, G., Zibuschka, F. and Puxbaum, H. (2003). Airborne bacteria as cloud condensation nuclei. *J. Geophys. Res.* 108: 4658.
- Bi, X., Liang, S. and Li, X. (2013). A novel in situ method for sampling urban soil dust: Particle size distribution, trace metal concentrations, and stable lead isotopes. *Environ. Pollut.* 177: 48–57.
- Biswas, K.F., Ghauri, B.M. and Husain, L. (2008). Gaseous and aerosol pollutants during fog and clear episodes in South Asian urban atmosphere. *Atmos. Environ.* 42: 7775–7785.
- Boone, E.J., Laskin, A., Laskin, J., Wirth, C., Shepson, P.B., Stirn, B.H. and Pratt, K.A. (2015). Aqueous processing of atmospheric organic particles in cloud water collected via aircraft sampling. *Environ. Sci. Technol.* 49: 8523–8530.
- Bower, K.N., Choularton, T.W., Gallagher, M.W., Beswick, K.M., Flynn, M.J., Allen, A.G., Davison, B.M., James, J.D., Robertson, L. and Harrison, R.M. (2000). ACE-2 HILLCLOUD. An overview of the ACE-2 ground-based cloud experiment. *Tellus Ser. B* 52: 750–778.
- Bowers, R.M., Clements, N., Emerson, J.B., Wiedinmyer, C., Hannigan, M.P. and Fierer, N. (2016). Seasonal variability in bacterial and fungal diversity of the near-surface atmosphere. *Environ. Sci. Technol.* 47: 12097–12106.

- Buchanan, R.E., Gibbons, N.E and Cowan, S.T. (1994). *Bergey's manual of determinative bacteriology*. Williams & Wilkins.
- Burrows, S.M., Elbert, W., Lawrence, M. and Pöschl, U. (2009). Bacteria in the global atmosphere—Part 1: Review and synthesis of literature data for different ecosystems. *Atmos. Chem. Phys.* 9: 9263–9280.
- Cao, C., Jiang, W., Wang, B., Fang, J., Lang, J., Tian, G., Jiang, J. and Zhu, T.F. (2014). Inhalable microorganisms in Beijing's PM_{2.5} and PM₁₀ pollutants during a severe smog event. *Environ. Sci. Technol.* 48: 1499–1507.
- Casalta, E. and Montel, M.C. (2008). Safety assessment of dairy microorganisms: The Lactococcus genus. *Int. J. Food Microbiol.* 126: 271–273.
- Collett, J., Iovinelli, R. and Demoz, B. (1995). A three-stage cloud impactor for size-resolved measurement of cloud drop chemistry. *Atmos. Environ.* 29: 1145–1154.
- Collett, J.L., Hoag, K.J., Sherman, D.E., Bator, A. and Richards, L.W. (1998). Spatial and temporal variations in San Joaquin Valley fog chemistry. *Atmos. Environ.* 33: 129–140.
- Demoz, B., Collett, J. and Daube, B. (1996). On the Caltech active strand cloudwater collectors. *Atmos. Res.* 41: 47–62.
- Deng, C., Zhuang, G., Huang, K., Li, J., Zhang, R., Wang, Q., Liu, T., Sun, Y., Guo, Z. and Fu, J. (2011). Chemical characterization of aerosols at the summit of Mountain Tai in Central East China. *Atmos. Chem. Phys.* 11: 7319–7332.
- Elbert, W., Taylor, P., Andreae, M. and Pöschl, U. (2007). Contribution of fungi to primary biogenic aerosols in the atmosphere: Wet and dry discharged spores, carbohydrates, and inorganic ions. *Atmos. Chem. Phys.* 7: 4569–4588.
- Evans, C.A., Coombes, P.J., Dunstan, R.H. and Harrison, T. (2009). Extensive bacterial diversity indicates the potential operation of a dynamic micro-ecology within domestic rainwater storage systems. *Sci. Total Environ.* 407: 5206–5215.
- Fahlgren, C., Bratbak, G., Sandaa, R.A., Thyrhaug, R. and Zweifel, U. (2011). Diversity of airborne bacteria in samples collected using different devices for aerosol collection. *Aerobiologia* 27: 107–120.
- Fomba, K.W., Van Pinxteren, D., Müller, K., Iinuma, Y., Lee, T., Collet, J. and Herrmann, H. (2015). Trace metal characterization of aerosol particles and cloud water during HCCT 2010. *Atmos. Chem. Phys.* 15: 10899–10938.
- Forstrom, R.J. and Wardle, M.D. (1980). *Cold gas sterilization process using hydrogen peroxide at low concentrations*. US.
- Gou, H., Lu, J., Li, S., Tong, Y., Xie, C. and Zheng, X. (2016). Assessment of microbial communities in PM₁ and PM₁₀ of Urumqi during winter. *Environ. Pollut.* 214: 202–210.
- Guo, J., Wang, Y., Shen, X., Wang, Z., Lee, T., Wang, X., Li, P., Sun, M., Collett, J.L. and Wang, W. (2012). Characterization of cloud water chemistry at Mount Tai, China: Seasonal variation, anthropogenic impact, and cloud processing. *Atmos. Environ.* 60: 467–476.
- Hao, L., Romakkaniemi, S., Kortelainen, A., Jaatinen, A., Portin, H., Miettinen, P., Komppula, M., Leskinen, A., Virtanen, A. and Smith, J.N. (2016). Aerosol chemical composition in cloud events by high resolution time-of-flight aerosol mass spectrometry. *Environ. Sci. Technol.* 47: 2645–2653.
- Hoag, K.J., Collett Jr, J.L. and Pandis, S.N. (1999). The influence of drop size-dependent fog chemistry on aerosol processing by San Joaquin Valley fogs. *Atmos. Environ.* 33: 4817–4832.
- Hoyle, C.R., Fuchs, C., Järvinen, E., Saathoff, H., Dias, A., El Haddad, I., Gysel, M., Coburn, S.C., Tröstl, J. and Bernhammer, A.K. (2015). Aqueous phase oxidation of sulphur dioxide by ozone in cloud droplets. *Atmos. Chem. Phys.* 15: 33843–33896.
- Huijnen, V., Williams, J.E. and Flemming, J. (2014). Modeling global impacts of heterogeneous loss of HO₂ on cloud droplets, ice particles and aerosols. *Atmos. Chem. Phys.* 14: 8575–8632.
- Hutchings, J.W., Robinson, M.S., McIlwraith, H., Kingston, J.T. and Herckes, P. (2009). The chemistry of intercepted clouds in Northern Arizona during the North American monsoon season. *Water Air Soil Pollut.* 199: 191–202.
- Joly, M., Amato, P., Deguillaume, L., Monier, M., Hoose, C. and Delort, A.M. (2014). Direct quantification of total and biological ice nuclei in cloud water. *Atmos. Chem. Phys.* 14: 3707–3731.
- Kaushik, R., Balasubramanian, R. and Dunstan, H. (2013). Microbial quality and phylogenetic diversity of fresh rainwater and tropical freshwater reservoir. *PLoS One* 9: e100737.
- Kourtev, P.S., Hill, K.A., Shepson, P.B. and Konopka, A. (2011). Atmospheric cloud water contains a diverse bacterial community. *Atmos. Environ.* 45: 5399–5405.
- Kovatch, J. and Schultz, G.E. (2013). Bacterial diversity in a large, temperate, heavily modified river, as determined by pyrosequencing. *Aquat. Microb. Ecol.* 70: 196–179.
- Lee, J.U. (2015). Antimony-oxidizing bacteria isolated from antimony-contaminated sediment – A phylogenetic study. *Geomicrobiol. J.* 32: 50–58.
- Li, P., Li, X., Yang, C., Wang, X., Chen, J. and Collett, J.L. (2011). Fog water chemistry in Shanghai. *Atmos. Environ.* 45: 4034–4041.
- Li, T., Wang, Y., Li, W.J., Chen, J.M., Wang, T. and Wang, W.X. (2015). Concentrations and solubility of trace elements in fine particles at a mountain site, southern China: Regional sources and cloud processing. *Atmos. Chem. Phys.* 15: 13001–13042.
- Liu, Q., Guo, H., Li, Y. and Xiang, H. (2013). Acclimation of arsenic-resistant Fe(II)-oxidizing bacteria in aqueous environment. *Int. Biodeterior. Biodegrad.* 76: 86–91.
- Liu, X.H., Wai, K.M., Wang, Y., Zhou, J., Li, P.H., Guo, J., Xu, P.J. and Wang, W.X. (2012). Evaluation of trace elements contamination in cloud/fog water at an elevated mountain site in Northern China. *Chemosphere* 88: 531–541.
- Lorenz, N., Hintemann, T., Kramarewa, T., Katayama, A., Yasuta, T., Marschner, P. and Kandeler, E. (2006).

- Response of microbial activity and microbial community composition in soils to long-term arsenic and cadmium exposure. *Soil Biol. Biochem.* 38: 1430–1437.
- Loubinoux, J., Mihaila-Amrouche, L., Le, F.A., Pigne, E., Huchon, G., Grimont, P.A. and Bouvet, A. (2003). Bacteremia caused by *Acinetobacter ursingii*. *J. Clin. Microbiol.* 41: 1337–1338.
- Menon, S., Saxena, V.K. and Logie, B.D. (2000). Chemical heterogeneity across cloud droplet size spectra in continental and marine air masses. *J. Appl. Meteorol.* 39: 887–903.
- Morris, C.E., Sands, D.C., Vinatzer, B.A., Glaux, C., Guilbaud, C., Buffière, A., Yan, S., Dominguez, H. and Thompson, B.M. (2008). The life history of the plant pathogen *Pseudomonas syringae* is linked to the water cycle. *ISME J.* 2: 321–334.
- Norberg, A.B. and Molin, N. (1983). Toxicity of cadmium, cobalt, uranium and zinc to *Zoogloea ramigera*. *Water Res.* 17: 1333–1336.
- Notholt, J., Hjorth, J. and Raes, F. (1992). Formation of HNO₂ on aerosol surfaces during foggy periods in the presence of NO and NO₂. *Atmos. Environ.* 26: 211–217.
- Peccia, J. and Hernandez, M. (2006). Incorporating polymerase chain reaction-based identification, population characterization, and quantification of microorganisms into aerosol science: A review. *Atmos. Environ.* 40: 3941–3961.
- Peng, Z. (2015). *Chemical characterization of cloud water from whiteface mountain, NY*. Thesis, University of Michigan.
- Peter, H., Hörtnagl, P., Reche, I. and Sommaruga, R. (2014). Bacterial diversity and composition during rain events with and without Saharan dust influence reaching a high mountain lake in the Alps. *Environ. Microbiol. Rep.* 6: 618–624.
- Plessow, K., Acker, K., Heinrichs, H. and Möller, D. (2001). Time study of trace elements and major ions during two cloud events at the Mt. Brocken. *Atmos. Environ.* 35: 367–378.
- Pratt, K.A., DeMott, P.J., French, J.R., Wang, Z., Westphal, D.L., Heymsfield, A.J., Twohy, C.H., Prenni, A.J. and Prather, K.A. (2009). In situ detection of biological particles in cloud ice-crystals. *Nat. Geosci.* 2: 398–401.
- Raja, S., Raghunathan, R., Yu, X.Y., Lee, T., Chen, J., Kommalapati, R.R., Murugesan, K., Shen, X., Qingzhong, Y., Valsaraj, K.T. and Collett Jr, J.L. (2008). Fog chemistry in the Texas–Louisiana Gulf Coast corridor. *Atmos. Environ.* 42: 2048–2061.
- Raja, S., Raghunathan, R., Kommalapati, R.R., Shen, X., Collett, J.L. and Valsaraj, K.T. (2009). Organic composition of fogwater in the Texas–Louisiana gulf coast corridor. *Atmos. Environ.* 43: 4214–4222.
- Redford, A.J., Bowers, R.M., Knight, R., Yan, L. and Fierer, N. (2010). The ecology of the phyllosphere: Geographic and phylogenetic variability in the distribution of bacteria on tree leaves. *Environ. Microbiol.* 12: 2885–2893.
- Seenivasagan, R., Kasimani, R., Rajakumar, S., Kalidoss, R. and Ayyasamy, P.M. (2016). Comparative modelling and molecular docking of nitrate reductase from *Bacillus weihenstephanensis* (DS45). *J. Taibah Univ. Sci.* 10: 621–630.
- Segata, N., Izard, J., Waldron, L., Gevers, D., Miropolsky, L., Garrett, W.S. and Huttenhower, C. (2011). Metagenomic biomarker discovery and explanation. *Genome Biol.* 12: 1–18.
- Shintani, H. (2009). Application of vapor phase hydrogen peroxide sterilization to endoscope. *Biocontrol Sci.* 14: 39–45.
- Spiegel, J., Aemisegger, F., Scholl, M., Wienhold, F., Collett Jr, J., Lee, T., Pinxteren, D.v., Mertes, S., Tilgner, A. and Herrmann, H. (2012). Stable water isotopologue ratios in fog and cloud droplets of liquid clouds are not size-dependent. *Atmos. Chem. Phys.* 12: 9855–9863.
- Straub, D.J. and Collett Jr, J.L. (2002). Development of a multi-stage cloud water collector Part 2: Numerical and experimental calibration. *Atmos. Environ.* 36: 45–56.
- Väitilingom, M., Attard, E., Gaiani, N., Sancelme, M., Deguillaume, L., Flossmann, A.I., Amato, P. and Delort, A.M. (2012). Long-term features of cloud microbiology at the puy de Dôme (France). *Atmos. Environ.* 56: 88–100.
- Van Pinxteren, D., Fomba, K.W., Mertes, S., Müller, K., Spindler, G., Schneider, J., Lee, T., Collett, J.L. and Herrmann, H. (2016). Cloud water composition during HCCT-2010: Scavenging efficiencies, solute concentrations, and droplet size dependence of inorganic ions and dissolved organic carbon. *Atmos. Chem. Phys.* 16: 3185–3205.
- Wang, Y., Guo, J., Wang, T., Ding, A., Gao, J., Zhou, Y., Collett, J.L. and Wang, W. (2011). Influence of regional pollution and sandstorms on the chemical composition of cloud/fog at the summit of Mt. Taishan in northern China. *Atmos. Res.* 99: 434–442.
- Wang, Y., Yu, W., Pan, Y. and Wu, D. (2012). Acid neutralization of precipitation in Northern China. *J. Air Waste Manage. Assoc.* 62: 204–211.
- Wani, P.A., Khan, M.S. and Zaidi, A. (2007). Chromium reduction, plant growth-promoting potentials, and metal solubilization by *Bacillus* sp. isolated from alluvial soil. *Curr. Microbiol.* 54: 237–243.
- Weller, C. and Herrmann, H. (2015). Kinetics of nitrosamine and amine reactions with NO₃ radical and ozone related to aqueous particle and cloud droplet chemistry. *Atmos. Res.* 151: 64–71.
- Whalley, L.K., Stone, D., George, I.J., Mertes, S., Van Pinxteren, D., Tilgner, A., Herrmann, H., Evans, M.J. and Heard, D.E. (2015). The influence of clouds on radical concentrations: Observations and modelling studies of HO_x during the Hill Cap Cloud Thuringia (HCCT) campaign in 2010. *Atmos. Chem. Phys.* 15: 3289–3301.
- Xu, C., Wei, M., Chen, J., Sui, X., Zhu, C., Li, J., Zheng, L., Sui, G., Li, W. and Wang, W. (2016). Investigation of diverse bacteria in cloud water at Mt. Tai, China. *Sci. Total Environ.* 580: 258–265.
- Yamaguchi, T., Katata, G., Noguchi, I., Sakai, S., Watanabe, Y., Uematsu, M. and Furutani, H. (2015). Long-term observation of fog chemistry and estimation

- of fog water and nitrogen input via fog water deposition at a mountainous site in Hokkaido, Japan. *Atmos. Res.* 151: 82–92.
- Zeng, J., Deng, L.J., Lou, K., Zhang, T., Yang, H.M., Shi, Y.W. and Lin, Q. (2014). Molecular characterization of the planktonic microorganisms in water of two mountain brackish lakes. *J. Basic Microbiol.* 54: 509–520.

Received for review, November 21, 2016

Revised, March 21, 2017

Accepted, March 25, 2017